APPLICATION OF A CRACK GROWTH MODEL TO SILICON NITRIDE

R. MOHRMANN and M. ROMBACH
Fraunhofer-Institut für Werkstoffmechanik, D-7800 Freiburg

ABSTRACT

The lifetime of ceramic specimens and components is commonly interpreted in terms of a theory, which is based on the presence of natural flaws like cracks and on the growth of these cracks according to $v = AK^n$ until fracture occurs (Wiederhorn, 1974; Evans and Fuller, 1974; Evans and Wiederhorn, 1974). The statistical scatter of strength and lifetime is related to the distribution of the initial flaw sizes. The Weibull distribution is usually used for a quantative description. Therefore, a basic concept is considered which allows to determine the reliability of ceramic components. The applicability of this concept has however to be proved.

In high strength ceramic, there is a rising crack resistance curve (R-curve effect) in addition to the time-dependent crack growth. It is assumed in the present paper that the R-curve effect is caused by bridges between the crack flanks (Knehans and Steinbrech, 1982), which unloads the actual crack tip. The formulation of the crack growth law is similar to that of Fett and Munz (1990). However, a different load-displacement equation of the bridges is proposed and verified as far as possible within the experimental results.

This theory is applied to macroscopic cracks and natural flaws in Si_3N_4. The model parameters were adjusted to the experiments on macroscopic cracks with numerical methods. The lifetimes of components containing natural flaws were estimated by integrating the crack growth law.

Keywords. R-curve, bridging, lifetime, natural flaws, silicon-nitride, crack growth.

EXPERIMENTAL

Material. A commercial sintered silicon nitride (SSN) was used. The measured mechanical properties at ambient temperature are compiled in Table 1.

Compliance Method. The growth of macroscopic cracks in 4-point bend specimens was investigated under ambient temperature, atmospheric conditions and different loading rates (0.001 MPa/sec to 1 MPa/sec). The crack length was calculated due to the compliance of the specimen. The (relative) loadline displacement was measured with a 3-point measurement device (resolution 0.01 μm).

Table 1. Material Properties.

spec. weight ρ [10^3 kg m^{-3}]	3,15
hardness H [GPa]	35
E-modulus [GPa]	283
G-modulus [GPa]	110
Poisson ratio ν	0,28
characteristic fracture strength σ_o [MPa]	535
Weibull modulus m	14,4

In-situ Experiments. In order to enable direct investigations of the crack growth and the mechanisms acting behind the crack tip an in-situ testing device for a scanning electron microscope (SEM) was built. This device works with 3-point bend specimens with a load cell based on strain gages and with a piezo actuator. Figure 1 shows the mounted in-situ testing device. The experiments can be performed with variable load cycles, and the tension surface as well as the side surface of the specimen can be observed.

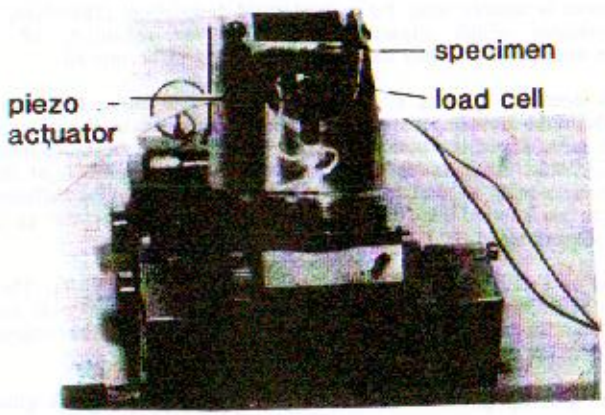

Fig. 1: Loading device for SEM investigations.

PHENOMENOLOGICAL CRACK GROWTH MODEL

The crack growth velocity $\dot{a}$ should be described as a function of the loading while bridges between the crack flanks are present. Figure 2 shows the model schematically. The crack flanks are bound by bridges until the crack opening displacement reaches the limiting value Δu_{max}. The bridges break above this value.

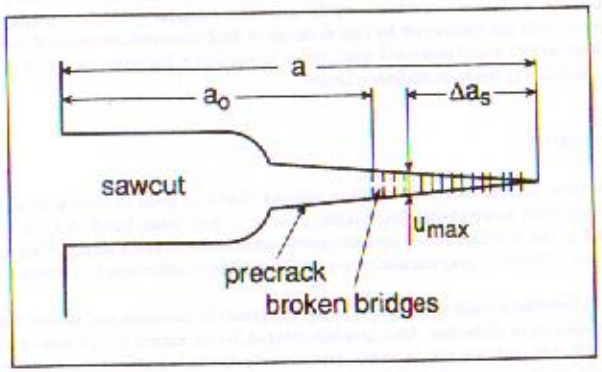

Fig. 2: Geometry of the model.

The stress intensity factor at the crack tip is given by

$$K_{tip} = K_{ext} - K_v \,, \tag{1}$$

where $K_{ext} = Y \sigma \sqrt{a}$ (2)

comes from the external stress σ (a = crack length, Y = geometry function) and K_v is the contribution caused by bridging. It is phenomenologically proposed to be

$$K_v = \begin{cases} Q(a-a_o) & a-a_o < \Delta a_s \\ Q\Delta a_s & a-a_o \geq \Delta a_s \end{cases} \tag{3}$$

Here, a_o is the inital crack length, and Q and Δa_s are parameters. Equation (3) describes the increase of the briding effects until a maximum value is reached with increasing crack length. The linear dependency was chosen in order to describe the experimental results approximately. Other functional dependencies are possible for different materials (Fett and Munz, 1990). An explanation of the linear increase will be given later with respect to the load-displacement equation of the bridges.

The crack velocity is described with the common power law depending on the crack tip stress-intensity factor

$$\dot{a} = A K_{tip}^{n} \,, \tag{4}$$

where A and n are material parameters.

In the case of time-independent crack growth the crack tip stress-intensity factor is equal to the critical value K_{Ic}. This leads to

$$K_{ext} = K_{Ic} + K_v \cdot \qquad (5)$$

In the case of time-dependent behaviour the crack growth law is numerically integrated with the Runge-Kutta method.

In order to adjust the model parameters to the experimental results, a fit routine, similar to the Levenberg-Marquardt algorithm (Press and Flanery, 1986), was established, where the numerical integration of the crack growth law is used as a subroutine of the fit routine.

RESULTS

Macrocracks. The measurements showed a strong increase of the crack resistance curve with increasing crack length. The results of two measurements in the SEM (vacuum, room temperature) are plotted in Fig. 3. Subcritical crack growth was not observed, therefore K_{tip} is equal to K_{Ic} for the points measured. The linear increase of K_{ext} with the crack extension can clearly be seen, which motivated the functional form of eq. (3).

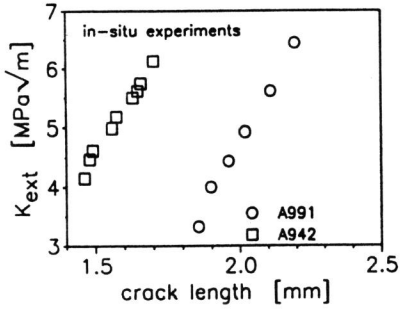

Fig. 3. Crack-resistance curves under vacuum.

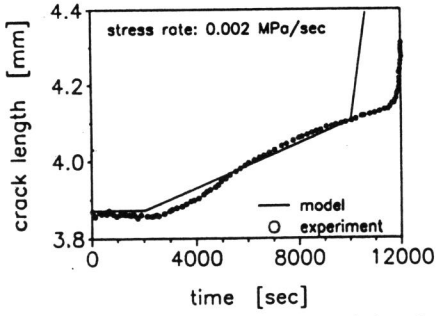

Fig. 4. Crack extension as a function of time in air.

Subcritical crack growth was observed under atmospheric conditions. In Fig. 4, the crack length is plotted as a function of time at a loading rate of 0.002 MPa/sec. A typical observation for all these experiments is a large region with approximately constant crack velocity. This is caused by the increasing crack resistance, K_v, while K_{ext} is increasing at the same time. Both effects nearly compensate each other. The model describes this situation well (Fig. 4).

Adjustment of Model Parameters. The value K_{Ic} was determined from K_{ext} at that time when first crack growth was indicated by the specimens compliance; K_{ext} had been measured in a fast bending test. The value is K_{Ic} = 2.0 MPa$\sqrt{m}$. The other model parameters, which were adjusted to crack growth experiments in vacuum (in SEM) and in air, are noted in Table 2.

In Fig. 5, the quality of this adjustment for two experiments on macrocracks under vacuum (SEM) is shown. The comparison for crack growth in air has already been given in Fig. 4.

Table 2: Material parameters (units: m, MPa).

experimental conditions	Q	Δa_s	A	n
air 4-point bending	7950	$380 \cdot 10^{-6}$	10^{-45}	150
vacuum 3-point bending	8560	$520 \cdot 10^{-6}$	-	-

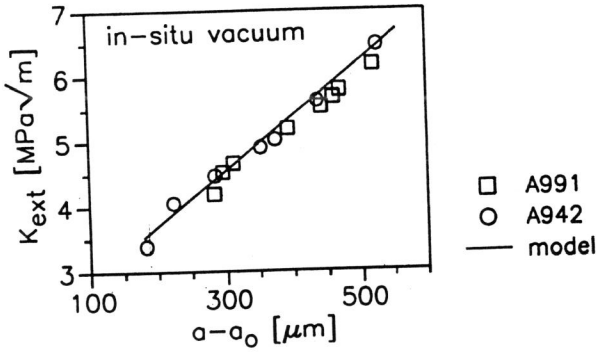

Fig. 5: Unique R-curve for two experiments.

Application of K_{Ic} to Natural Flaws. In Fig. 6, the fractographically determined sizes of the fracture origins in 4-point bending specimens (without macroscopic

crack) are plotted. The line gives the relation between the fracture stress and the size of the fracture origin for a surface crack (Y = 1.28) at K_{Ic} = 2.0 MPa$\sqrt{m}$. All the measured fracture stresses are above this theoretical line. This should be expected because pore-like failures cause a lower stress concentration than cracks do.

Bridging and Crack Opening Displacement. The reason for the rising crack resistance curve is the growth of a bridging zone behind the crack tip. The bridging zone arises typically at slow controlled crack growth, but not along a fast growing crack. This corresponds to the result that the crack resistance at the beginning of controlled crack growth is independent of the initial crack length because the inital cracks were popped in. Two different types of bridging effects can be found: Spring-like bridges (see Fig. 7a) are dominating. Bridges, which look like causing friction (Fig. 7b) are less frequent.

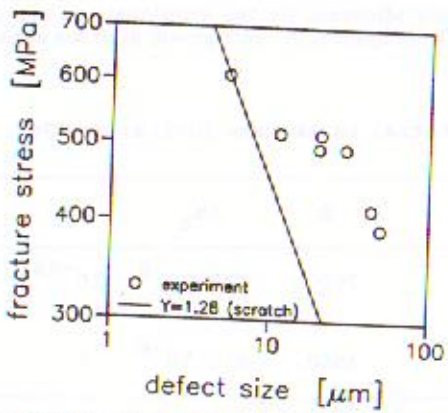

Fig. 6. Comparison of the fracture-mechanical relation with experimental data and natural flaws.

a) left b) right

Fig. 7. SEM photographs of bridges.

The crack opening displacement Δu was measured as a function of the distance x from the crack tip in the SEM. The result is given by the following adjusted equation:

$$\Delta u(x) = \frac{8.4\ (1-\nu^2)\ K_{Ic}}{(\pi/2)^{1/2}\ E}\sqrt{x}\ . \qquad (6)$$

Figure 8 shows the experimental results and the curve calculated with eq. (6).

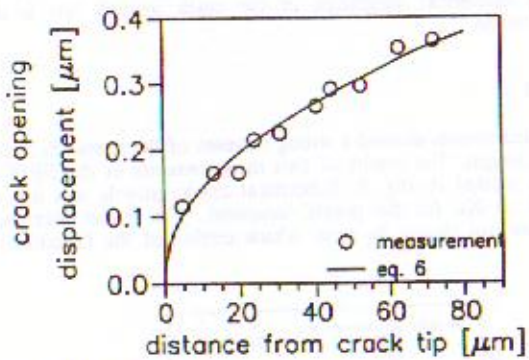

Fig. 8. Measured crack-opening displacement and eq. (6).

The load-displacement equation for the bridges should be estimated from the macroscopic behaviour. The load, which is transmitted by the bridges, is assumed to be a continuous function of the relative displacement of the crack flanks u. The influence of the bridges to the stress intensity factor is

$$K_v = \int_0^{a-a_0} g(x,a)\ \sigma_v[u(x)]\ dx\ , \qquad (7)$$

where x is the distance from the crack tip and g(x,a) is a weight function. In the case of a small bridging zone, compared to the crack length, $g(x,a) = (\pi x/2)^{-1/2}$ is valid. Otherwise, g(x,a) depends of the specimen geometry and is given for bending specimens after Fett and Munz (1990).

Equation (5) is only compatible to the phenomenological eq. (3), if the integrand is neither dependent on x nor on a. This is the case only, if $\sigma_v \propto \sqrt{x}$ and under the assumption of a small bridging zone ($g \propto 1/\sqrt{x}$). This leads to a linear relation between σ_v and Δu

$$\sigma_v(u) = \begin{cases} \dfrac{\pi\ Q\ E}{16\cdot 8(1-\nu^2)\ K_{Ic}}\ \Delta u & \text{for } \Delta u < \Delta u_{max} \\ 0 & \text{for } \Delta u > \Delta u_{max}\ . \end{cases} \qquad (8)$$

The maximum value Δu_{max}, where the bridges fail, is given by eq. (3) with $x = \Delta a_s$.

The arguments, which lead to eq. (6) are not theoretically consistent. From a fracture-mechanical point of view, the crack-opening displacement u(x) differs from the square-root dependence on x in presence of stresses along the crack flanks. The exact description would require the (numerical) solution of an integral equation. At least, eq. (6) describes the crack-opening displacement good enough concerning the measurement errors, and load-displacement equations, strongly differing from eq. (8), will not correspond to the measured results of eqs. (3) and (6).

Lifetime calculation for short cracks. In Fig. 9, the calculated lifetime is plotted for various initial crack lengths. The parameters, which were presented before, were used for the crack growth law. Bridging effects were neglected (Q = 0) because they have no significant influence. Therefore, the small cracks do not take credit from the R-curve effect in this materials.

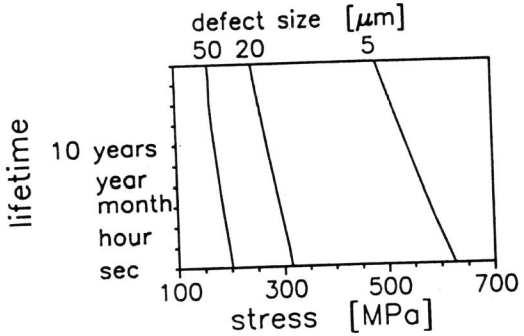

Fig. 9. Calculated lifetimes.

CONCLUSION

A pronounced R-curve was found for silicon nitride, which results from bridging effects behind the crack tip. A fracture-mechanical model was established taking bridging effects as well as slow crack growth into account. It turned out that there is only a material-dependent load-displacement equation for the bridging, but no unique R-curve.

REFERENCES

Evans, A.G., and E.R. Fuller (1974), Crack Propagation in Ceramic Materials Under Cyclic Loading Conditions, Metall. Trans. **5**, 27-33.
Evans, A.G., and S.M. Wiederhorn (1974), Proof-Testing of Ceramic Materials - An Analytical Basis for Failure Prediction, Int. J. Fracture **11**, 379-392.
Fett, T., and D. Munz (1990), Influence of Crack Surface Interactions on Stress Intensity Factors in Ceramics, J. Mat. Sci. Letters **9**, 1403-1406.
Knehans, R., and R. Steinbrech (1982), Memory Effects of Crack Resistance During Slow Crack Growth in Notched Al_2O_3 Bend Specimens, J. Mater. Sci. Letters **1**,327-329.
Press, W.H., and B. Flanery (1986), Numerical Recipes, Cambridge University Press.
Wiederhorn, S.M. (1974), Reliability, Life Prediction and Proof-Testing of Ceramics, in: Ceramics for High-Performance Applications, J.J. Burke, A.E. Gorum, R.N. Katz, Eds., Chestnut Hill, 633-663.
Mohrmann, R., M. Rombach, H. Riedel (1992), Anwendung eines Rißwachstumsmodells auf Siliziumnitrid, IWM-Bericht M 3/92, Freiburg.